# Modeling of Gas Compressors and Hierarchical Reduction for Globally Convergent Stationary Network Solvers

Tanja Clees, Igor Nikitin, Lialia Nikitina, Łukasz Segiet
Fraunhofer Institute for Algorithms and Scientific Computing
Sankt Augustin, Germany
Email: {Tanja.Clees|Igor.Nikitin|Lialia.Nikitina|Lukasz.Segiet}@scai.fraunhofer.de

***Abstract*—Further development on globally convergent algorithms for solution of stationary network problems is presented. The algorithms make use of global non-degeneracy of Jacobi matrix of the system, composed of Kirchhoff's flow conservation conditions and transport element equations. This property is achieved under certain monotonicity conditions on element equations and guarantees an existence of a unique solution of the problem as well as convergence to this solution from an arbitrary starting point. In application to gas transport networks, these algorithms are supported by a proper modeling of gas compressors, based on individually calibrated physical characteristics. This paper extends the modeling of compressors by hierarchical methods of topological reduction, combining the working diagrams for parallel and sequential connections of compressors. Estimations are also made for application of topological reduction methods beyond the compressor stations in generic network problems. Efficiency of the methods is tested by numerical experiments on realistic networks.**

***Keywords–modeling of complex systems; topological reduction; globally convergent solvers; applications; gas transport networks.***

## I. INTRODUCTION

This work is an extension of our conference paper [1], concentrated on mathematical modeling of single gas compressors in the context of designing globally convergent network solvers. Here we will add the modeling of aggregate compressor stations, obtained from the single compressors by parallel and sequential connections. We perform topological reduction of the stations, by combining the individually calibrated physical profiles of compressors into a cumulative profile, representing the compressor station as a single element. We will also estimate a benefit of generic topological reduction algorithms for generic networks and perform more numerical experiments for this purpose.

The simulation of transport networks in civil engineering has become increasingly important for the planning and stable operation of modern infrastructure. Compressors are essential elements in gas transport networks; they create pressure necessary for driving gas towards the consumers. A mathematical modeling of gas compressors should take into account their individually calibrated physical profiles. Our approach is based on conversion of the measured profiles into an explicitly resolved form suitable for globally convergent solvers. In particular, a proper signature of derivatives for the element equation of a compressor is provided.

Earlier [2], we have shown that the solvers for generic stationary network problems can be made globally convergent under special conditions on modeling of their elements. Stationary network problems combine linear Kirchhoff's equations and (generally non-linear) element equations. The first class of equations represents conservation laws, the second class describes the transport. We have proven that under certain monotonicity conditions on element equations, i.e., a special signature of the derivatives, the whole system possesses a globally non-degenerate Jacobi matrix. As a result, the problem always has exactly one solution. Moreover, standard algorithms, like Armijo backtracking line search and Katzenelson piecewise linear tracing, provide convergence to this solution from an arbitrary starting point.

These ideas have been implemented in our multi-physics network simulator MYNTS as described in [3], [4]. Considering gas transport networks, these papers used a simplified modeling of gas compressors, known in the simulation community as *free compressors*. This type of compressors does not possess limits on their power, only input or output pressure or gas flow are restricted. The present work extends the modeling by realistic characteristics to so called *advanced compressors*. Such compressors are described by individually measured physical profiles, defining the limits on power, revolution number, working region, etc. We will show how to incorporate such realistic characteristics into our globally convergent solver.

Modeling of gas transport networks has been considered in full detail in paper [5]. The networks are composed of a variety of elements (pipes, valves, compressors, drives, regulators, resistors, etc.), each type possessing a particular element equation. For instance, the pressure drop in pipes is described either by an empiric quadratic law [6] or by more accurate formulae by Nikuradse [7] and Colebrook-White [8]. Compressors and regulators have a control logic, implemented in the form of control equations or inequalities [5], e.g., a compressor/regulator can have a control goal to keep fixed output pressure, input pressure or flow value. There are various models for compressors (turbo, piston) and their drives (gas turbine, steam turbine, gas motor, electro motor), with characteristic diagrams calibrated on real engines.

The nodal variables (pressure, density, temperature, etc.) are related by equations of state, including various gas laws (ideal, Papay, standards of the American Gas Association – AGA and the International Organization for Standardization – ISO [9], [10]). Gas composition is defined in terms of molar components and effective gas properties (critical temperature and pressure, calorific value, molar mass, etc.), with appropriate equations describing their propagation and mixing. Thermal modeling [5] includes a number of physical effects (non-linear heat capacity, heat exchange with the soil, Joule-Thomson effect, i.e., a temperature drop due to free expansion of gas through a valve, regulator, etc.).

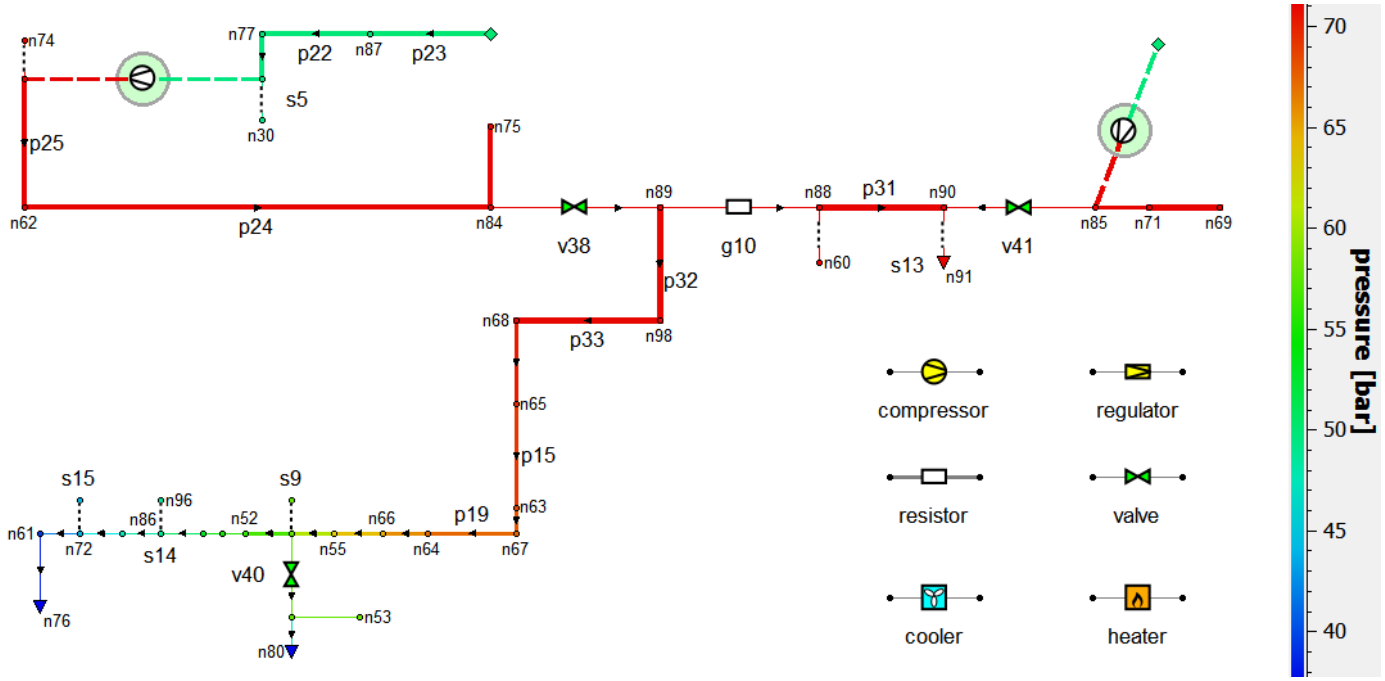


Figure 1. Test gas transport network N1 with 100 nodes, 111 edges.

The obtained system of equations and inequalities is solved by non-linear programming methods [11], [12]. Due to the non-linearity of equations, the stability of the solver critically depends on the choice of the starting point. For this purpose, various empirical strategies are used [13], [14]. An alternative has been proposed in our papers [2], [3], employing globally convergent algorithms, able to find the solution from an arbitrary starting point.

Topological reduction methods of the network utilizing the elimination of parallel and sequential connections are based on the concept of series-parallel graph (SPG, [15]). This is the graph reducible to a single edge by repeated application of such operations. Further extension is a generalized series-parallel graph (GSPG, [16]), where in addition to the elimination of parallel and sequential connections one can eliminate a leaf (node of valency 1). SPGs and GSPGs are recognizable in linear time with respect to the size of the graph, or in logarithmic time using a linear number of parallel processors. Decomposition of such graphs to elementary components is also performed in linear time, as well as solution of many other graph-theoretical problems, which would be NP-complete for generic graphs [17–19]. In our application, the concepts of SPGs and GSPSs are of key importance, since they allow essential reduction of the networks to an irreducible skeleton with small number of elements. The solver should be applied only to the skeleton, while the complete solution can be reconstructed with simple algorithms using the reduction history. The efficiency of such reduction for generic networks will be studied in this paper.

In Section II, we recall conditions on the generic stationary network problem, necessary for global convergence, and concretize these conditions in application to gas transport networks. In Section III, we describe modeling of advanced gas compressors. In Section IV, we present our implementation of modeling, which fulfills the conditions for global convergence. In Section V, we describe topological reduction algorithms for gas compressor stations and in Section VI generalize them to arbitrary elements and network types. In Section VII, we present numerical experiments with a number of realistic gas transport network examples and discuss the results obtained.

## II. Global convergence and gas transport networks

A generic stationary network problem can be written as

$$\sum_e I_{ne} Q_e = Q_n^{(s)},\ n \notin N_P,\ P_n = P_n^{(s)},\ n \in N_P,$$
$$f_e(P_{in}, P_{out}, Q_e) = 0, \quad (1)$$

where indices $n = 1...N$ denote the nodes and $e = 1...E$ the edges of the associated network graph, $I_{ne}$ is an incidence matrix of the graph, $Q_e$ are flows through the edges, $Q_n^{(s)}$ are source/sink contributions, localized in supply/exit nodes, $P_n$ are nodal variables (pressure for gas transport networks), $P_n^{(s)}$ are set values, localized in the subset $N_P$ of supply/exit nodes, at least one value per connected component of the graph. Let the element equations possess derivatives of the signature:

$$\partial f_e/\partial P_{in} > 0,\ \partial f_e/\partial P_{out} < 0,\ \partial f_e/\partial Q_e < 0. \quad (2)$$

It has been proven in [2] that the system (1) under condition (2) possesses a globally non-degenerate Jacobi matrix.

Gas transport networks, e.g., the networks shown in Figure 1, consist of several types of elements, all possessing the property (2). The gas networks are mostly composed of pipes with a non-linear (nearly quadratic) element equation. Some elements (valves and shortcuts) have linear equations, most complex elements (compressors and regulators) possess piecewise linear equations. According to [14], all continuous

piecewise linear functions can be represented in a max-min form:

$$f(x) = \max_i \min_j \sum_k a_{ijk} x_k + b_{ij}, \quad (3)$$

where $a, b$ are coefficient lists. In particular, free compressors are described by the following element equation:

$$\max(\min(\ P_{in} - P_L, -P_{out} + P_H, -Q + Q_H), \quad (4)$$
$$P_{in} - P_{out}, -Q) + \epsilon(P_{in} - P_{out} - Q) = 0.$$

The compressor tries to satisfy one of the following control goals:

- a specified pressure on output (SPO);
- a specified pressure on input (SPI);
- a specified mass flow (SM).

Being combined with the given upper and lower bounds:

$$\begin{aligned} P_H &= \min(SPO, POMAX), \\ P_L &= \max(SPI, PIMIN), \\ Q_H &= \min(SM, MMAX), \end{aligned} \quad (5)$$

the element equation defines a polyhedral surface shown in Figure 2, top. Here, $P_H$ stands for high pressure limit, $P_L$ – low pressure limit, $Q_H$ – high flow limit; $POMAX$ is an upper safety bound on output pressure, $PIMIN$ is a lower safety bound on input pressure, $MMAX$ is an upper safety bound on the flow.

Every face of the diagram corresponds to the best possible fulfillment of the control goal, e.g., $P_{out} = P_H$ (typical for SPO-mode), $Q = Q_H$ (typical for SM-mode), $P_{in} = P_{out}$ (bypass BP, equivalent to an open valve), $Q = 0$ (OFF, equivalent to a closed valve), etc. A small $\epsilon$ value is used for regularization purposes.

Every compressor is part of a compressor station, the simplest one is shown in Figure 2, bottom. This figure presents a compressor station with one machine unit, including (in flow direction) input resistor, compressor, cooler, output resistor, exit valve, (in an oblique direction) bypass valve, bypass regulator, both currently closed. In more complex stations, the compressors with accompanying elements are cascaded to parallel or sequential configurations, see Figure 3.

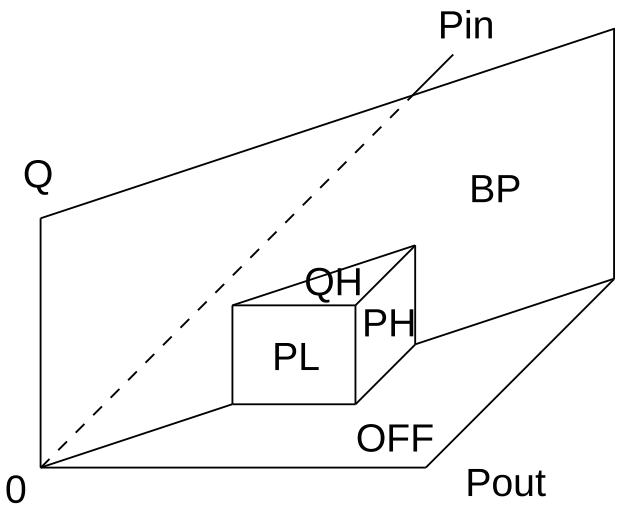


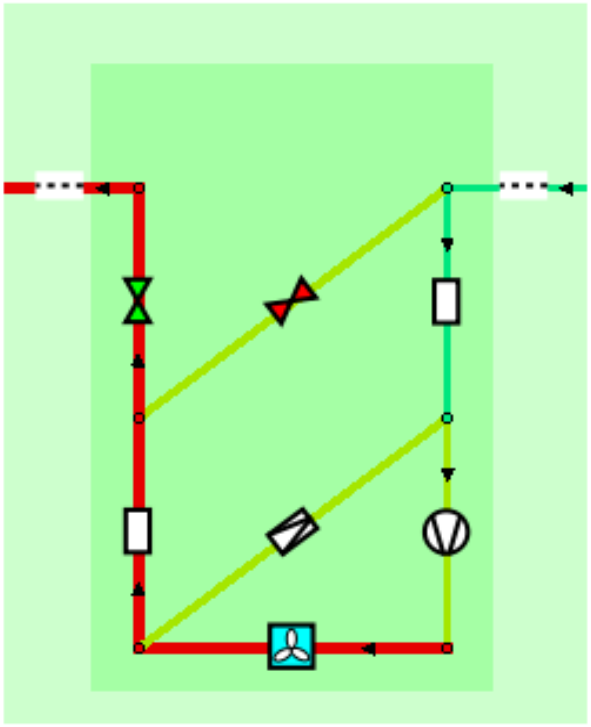

Figure 2. On the top: control diagram of free compressor. On the bottom: a compressor station with one machine unit.

## III. Advanced Modeling of Gas Compressors

In addition to pressure $P$, the nodes in gas transport networks possess other common variables, including: $\rho$ – mass density, $T$ – temperature, $z$ – compressibility factor, $\mu$ – molar mass.

In addition to conserving mass flow $Q$, measured in kg/s, sometimes volume flow $Q_x$ is also considered. It is measured in m$^3$/s with explicit reference to the measurement conditions, e.g., $Q_{norm}$ represents the volume flow under normal conditions (1 bar, 273.15 K), $Q_{in,out}$ refers to the volume flow under conditions in the input and output nodes. Different flow definitions are related by the formula:

$$Q = Q_{norm}\rho_{norm} = Q_{in}\rho_{in} = Q_{out}\rho_{out}. \quad (6)$$

Advanced compressors bring four new variables: $H_{ad}$ – adiabatic enthalpy increase, $\eta_{ad}$ – adiabatic efficiency, $r$ – revolution number of compressor drive, $W$ – power of compressor drive. Also, four equations are added [5]:

$$\begin{aligned} H_{ad} &= RT_{in}z_{in}/(\mu\alpha) \cdot ((P_{out}/P_{in})^{\alpha} - 1)\,, \\ W &= QH_{ad}/\eta_{ad}, \\ H_{ad} &= (1, r, r^2) \cdot A \cdot (1, Q_{in}, Q_{in}^2)^T, \\ \eta_{ad} &= (1, r, r^2) \cdot B \cdot (1, Q_{in}, Q_{in}^2)^T, \end{aligned} \quad (7)$$

where $R$ is the universal gas constant, $\kappa$ the adiabatic exponent, $\alpha = (\kappa - 1)/\kappa$. $A$ and $B$ are (3x3)-matrices filled with calibration constants. In addition, working limits for compressors

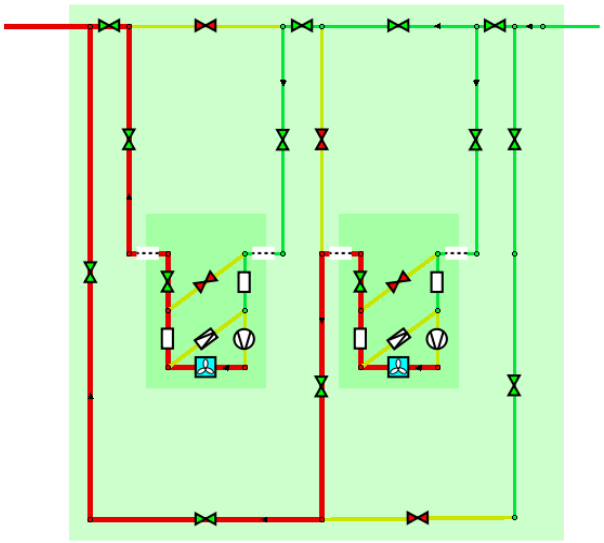

Figure 3. A compressor station with two machine units in parallel configuration.

are defined by the following inequalities:

$$\begin{aligned} & r_{min} \le r \le r_{max},\ \eta_{ad} \ge \eta_{min}, \\ & Q_{in} \ge Q_{min},\ W \le W_{max}, \\ & Q_{min} = (1, H_{ad}, H_{ad}^2) \cdot C^T, \\ & W_{max} = (1, r, r^2) \cdot D^T, \end{aligned} \tag{8}$$

where the constants $r_{min}$, $r_{max}$ define limits of the revolution number, $\eta_{min}$ – the lower limit on efficiency (so called choke line); $Q_{min}$ is a lower limit on the input volume flow (a surge line), $W_{max}$ is an upper limit on power. $C$, $D$ are (3)-vectors filled with calibration constants.

The constants in $(A, B, C, D)$ are found by fitting the measured data for the compressor considered as part of a calibration procedure and further represent the individual profiles for this compressor. Here, we described the modeling for a common class of turbo compressors and gas turbine drive engines. The other types are simpler in implementation and can be modeled analogously.

Figure 4 (top) shows profiles for a typical turbo compressor. In this plot, the horizontal axis represents input volume flow $Q_{in}$, the vertical axis – adiabatic enthalpy increase $H_{ad}$. Solid blue curves are the lines of constant revolution number $r$, their uppermost curve corresponds to $r_{max}$, the lowest curve – to $r_{min}$. The red curve is the surge line $Q_{in} = Q_{min}$, while the rightmost cyan curve – the choke line $\eta_{ad} = \eta_{min}$. The points in this diagram depict the data measured, a blue cross denotes the current working point of the compressor.

The equations (7) serve as definitions of newly introduced variables, while the inequalities (8) define the restrictions, in addition to (4) of those for a free compressor. The upper bounds $r = r_{max}$ and $W = W_{max}$ define new upper bounds for the flow and should be combined with the one defined by the diagram for a free compressor, shown in Figure 2 top. The lower bounds $r = r_{min}$ and $Q_{in} = Q_{min}$ show the points where the station automatically opens its bypass

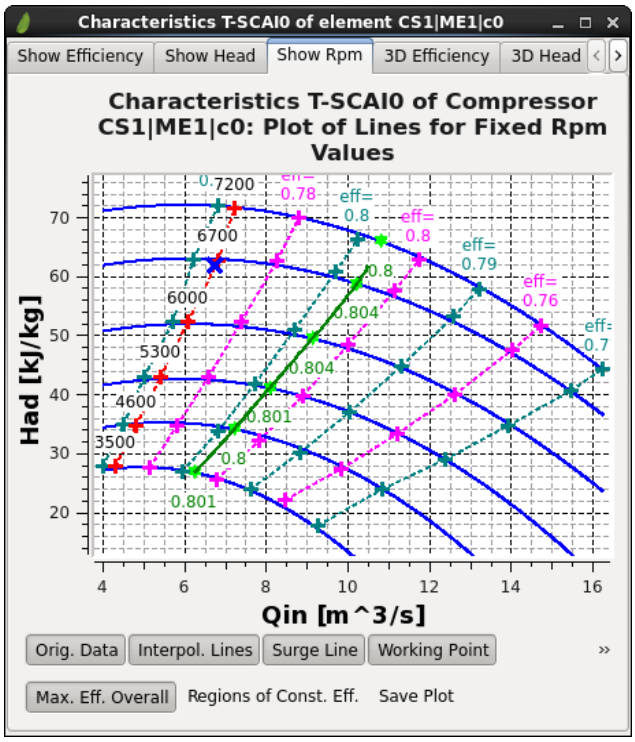


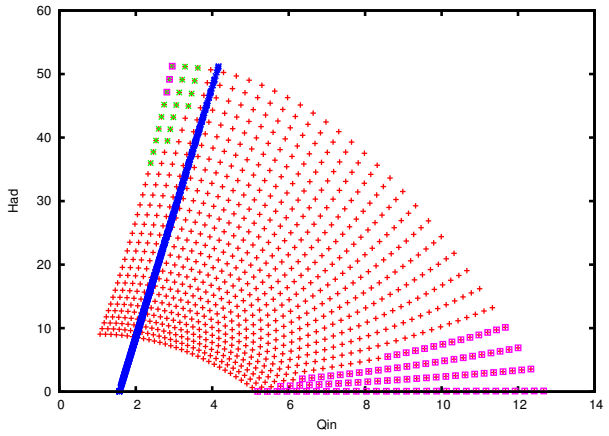


Figure 4. Advanced modeling of compressors. On the top: typical characteristic diagram. Solid blue curves are lines of constant revolution number. On the bottom: stability analysis.

regulator, shown in Figure 2 bottom. After that the gas starts to circulate inside the station, so that the compressor never violates its bounds. The choke line $\eta_{ad} = \eta_{min}$ cuts off a region of unstable calibration related with the small $\eta_{ad}$ in the denominator of (7). Usually, the working point of a compressor is not located in this region, except of the starting procedure. On necessity the diagram can be continued in this region by a convenient monotone formula.

If $P_{in}$ and $P_{out}$ are fixed and the compressor is on its $r = r_{max}$ limit, it is straightforward to resolve the equations analytically, finding $H_{ad}$, $Q_{in}$, $\rho_{in}$, $Q$, $\eta_{ad}$ and $W$, in this order. If $r$ and $Q_{in}$ are fixed and the compressor is on its $W = W_{max}$ limit, the equations can be resolved in

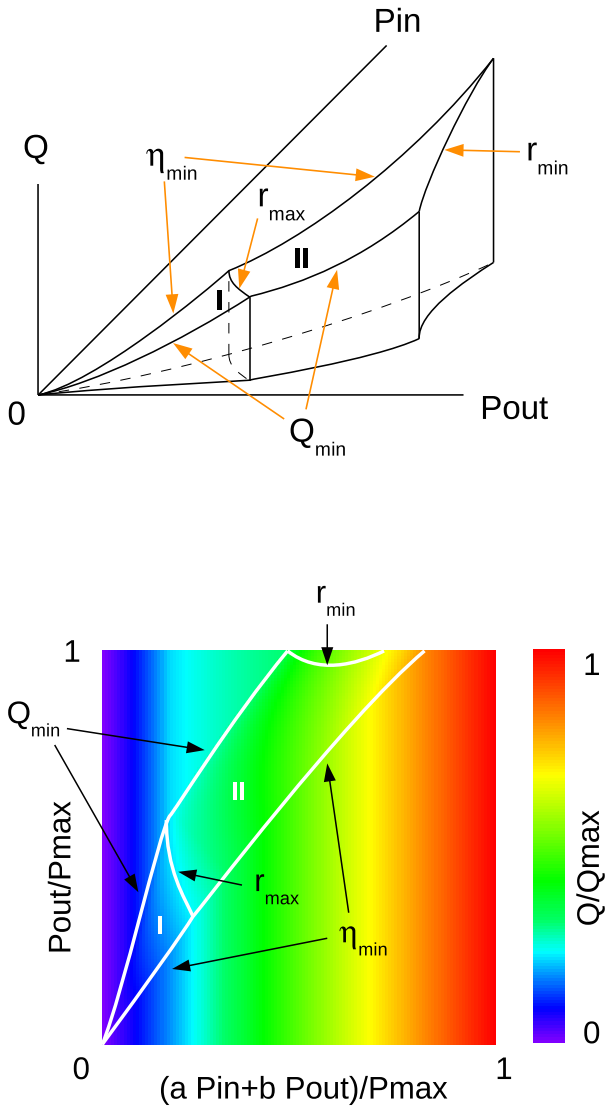


Figure 5. Advanced modeling of compressors (cont'd). On the top: control diagram of an advanced compressor. On the bottom: the same diagram in affine coordinates and color map representation.

the order $H_{ad}$, $\eta_{ad}$, $W_{max}$, $Q$, $\rho_{in}$, $P_{in}$, $P_{out}$. The first analytic formula gives an explicit representation $Q(P_{in}, P_{out})$ for the surface, defining a patch of the element equation. The second one represents the other patch in a parametric form $(r, Q_{in}) \to (P_{in}, P_{out}, Q)$. By numerical differentiation, it is possible to find the normals to both surfaces, which directly define the signatures of the corresponding patches. We recall that the correct signature reads $(+--)$, see (2). In Figure 4 (bottom) green points show the area of wrong signature. The blue curve is the surge line, magenta points show the area $\eta_{ad} < \eta_{min}$. Normally, the unstable green area is cut off by the surge and choke lines, so that the whole working region of the compressor is stable. In rare cases, when it is not so, the surge and choke lines should be modified accordingly.

## IV. Globally convergent implementation

Figure 5 (top) shows the surface $Q_{adv}(P_{in}, P_{out})$ defined by the characteristics of the advanced compressor. The calibrated part of the surface is located between the curves $Q_{min}$ and $\eta_{min}$ and consists of two patches I and II, connected on the $r_{max}$ line. Patch I is located between the $r_{max}$ line and the origin. Here, the input and output pressures are small and the compressor's performance is limited by its maximal revolution number: $r = r_{max}$. Patch II is located between the $r_{max}$ and $r_{min}$ lines. Here, the pressures are large and the compressor is limited by the maximal power of the drive: $W = W_{max}$. On $Q_{min}$ and $r_{min}$ curves the surface vertically falls down. This behavior corresponds to the open bypass regulator. $Q$ in that case denotes a total mass flow through the compressor and bypass regulator. The flow through the compressor remains equal to $Q_{min}$ or the equivalent flow on the $r_{min}$ line, while the negative difference $\Delta Q$ circulates through the bypass regulator. A slope of the vertically falling faces should be $\epsilon$-regularized to provide the necessary signature $(+--)$. The surface should be continued beyond $\eta_{min}$ curve by any function supporting the same signature.

Figure 5 (bottom) shows the same diagram as a color map. Patch II requires a conversion from parametric to explicit representation. For this purpose, we adopt resampling algorithms well known in computer graphics (CG). At first, we perform an affine transformation:

$$\begin{pmatrix} x \\ y \end{pmatrix} = \begin{pmatrix} a & b \\ 0 & 1 \end{pmatrix} \begin{pmatrix} P_{in} \\ P_{out} \end{pmatrix} \cdot \frac{1}{P_{max}}, \qquad (9)$$

with $a + b = 1$. The square on the $(x, y)$-plane is represented as a $N_{px} \times N_{px}$ pixel buffer, storing floating point values of $Q$ in double precision. Patches I and II are regularly sampled and represented as triangle strip sets. Then, the patches are rendered onto the $(x, y)$-plane using the Z-buffer algorithm. Finally, the remaining gaps are filled by copying a constant $Q$-value along the columns and to the right – by a linearly increasing function in the row. As a result, the $Q_{adv}$-function in these regions becomes dependent only on $x$. Monotonous increase of $Q$ on the border lines and a choice of affine coefficients $a > 0$, $b < 0$ support correct signature of the function $Q_{adv}(P_{in}, P_{out})$. If the bypass regulator is activated, the part above the upper border lines must be reset towards $Q = 0$, providing a regularized vertical fall of the surface on this bound.

The described algorithms provide a transformation from the calibration coefficients $(A, B, C, D)$ and characteristic diagram in Figure 4 (top) to the tabulated function $Q_{adv}(P_{in}, P_{out})$, represented by the color map in Figure 5 (bottom). This transformation should be done once per advanced compressor. For a moment, we use an implementation of the CG algorithms on Central Processing Unit (CPU) and plan their acceleration with Graphics Processing Unit (GPU).

In the solver, the lookup function $Q_{adv}(P_{in}, P_{out})$ is made available via rapid bilinear interpolation of tabulated values inside the $(x, y)$-square. It is continued to the whole $(x, y)$-plane by an explicit analytic formula:

$$f(x, y) = f(\hat{x}, \hat{y}) + k(\min(x, 0) + \max(x - 1, 0)), \quad (10)$$
$$\hat{x} = \min(\max(x, 0), 1), \quad \hat{y} = \min(\max(y, 0), 1),$$

with a constant $k > 0$. This global function is constructed similarly to the continuation formulas in [2]. In our special case it provides monotonous increase in $x$ and constancy in $y$ outside of the tabulated region.

Finally, the element equation for an advanced compressor is obtained by extending (4) as follows:

$$\begin{aligned}\max(\min(\ P_{in}-P_L, -P_{out}+P_H, -Q+Q_H,\\ \underline{Q_{adv}(P_{in},P_{out})-Q}), P_{in}-P_{out}, -Q)\\ +\epsilon(P_{in}-P_{out}-Q)=0.\end{aligned} \quad (11)$$

For clarity, the inserted term is underlined.

We have implemented the algorithms described above in our network simulator MYNTS in a preliminary version (solver strategy "stable").

## V. Modeling of Gas Compressor Stations

Machine units consisting of compressors and their drives are often combined in stations using parallel and sequential connections, such as shown in Figure 6. Parallel connections (Figure 6a,c) are used to increase throughput, while sequential connections (Figure 6b,d) allow to increase the output pressure in several steps. Mixed connections are also used, possessing various topologies (Figure 6e-g). In these figures, the compressor symbols represent single compressor stations (Figure 2), where the functional element is the compressor and the other elements serve mainly for flow switching.

The idea considered in this section is to combine the element equations of single compressors and to represent the station as a single element. At first, free diagrams depending on (SPO,SPI,SM) parameters should be unified with the advanced characteristics, so that the algorithms can operate on a single table per compressor. Then, the corresponding combination of lookup tables will describe the behavior of the station as a whole. This will reduce the number of equations in the system and will also allow to resolve certain stability issues.

Compressor stations bring unstable internal degrees of freedom, i.e., undefined balance of flows in parallel stations, undefined intermediate pressure in sequential stations. This instability is a particular case of the common singularity, for which $\epsilon$-regularization is used in the element equation (11). From a geometrical point of view, the hypersurfaces defined by the equations do not have a stable transversal intersection, but are in unstable tangent position.

The reason of this instability is the appearance of linear dependencies in the system matrix. For instance, two parallel SPO compressors set the same pressure value in the same output node, imposing two identical $P = SPO$ equations in the system. The system matrix becomes formally degenerate. Also, the fact that one equation is actually wasted leads to the effective reduction of the system size by one, so that one of the variables remains undefined. In this particular example, the undefined variable is the flow balance between the compressors. In the other case, namely a sequential connection of SM compressors, the $Q = SM$ equation is duplicate and the undefined variable is the intermediate pressure between the compressors.

The replacement of the station by a single element with combined characteristics removes internal degrees of freedom and improves stability of the numerical simulation.

Compressors, as well as all other elements are described by functions of the form: $Q(P_{in}, P_{out})$, or equivalently: $P_{out}(P_{in}, Q)$, $P_{in}(P_{out}, Q)$, where $Q$ is the mass flow, $P_{in}, P_{out}$ are input/output pressures. Monotonicity conditions

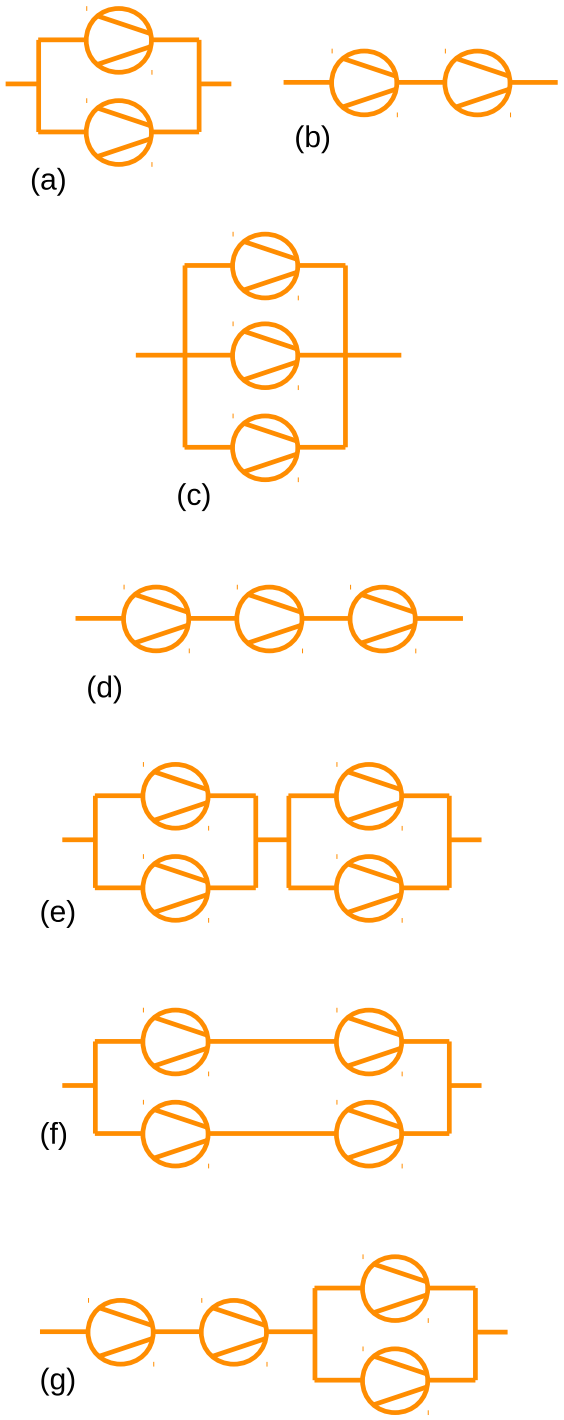


Figure 6. Examples of compressor stations: (a) parallel, (b) sequential, (c) 3 parallel, (d) 3 sequential, (e-g) mixed.

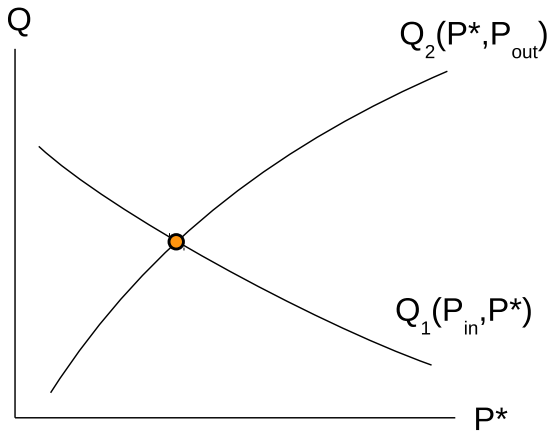


Figure 7. Equality of flows in sequential station has a single solution, due to monotonicity of element equations.

allow a unique inversion for any of these functions with respect to one of the arguments, passing from one representation to the other.

According to Kirchhoff's law, for connected elements $(1, 2)$ these functions can be combined as follows:

parallel connection:

$$Q(P_{in}, P_{out}) = Q_1(P_{in}, P_{out}) + Q_2(P_{in}, P_{out}); \quad (12)$$

sequential connection:

$$P_{out}(P_{in}, Q) = P_{out,2}(P_{out,1}(P_{in}, Q), Q). \quad (13)$$

Considering the monotonicity of the element equations, it is easy to verify that the combined elements possess correct signature of the derivatives, necessary for the global convergence. Indeed, the sum of monotonic functions in parallel connection is the monotonic function of the same signature. The composition of functions in sequential connection is monotonously increasing with $P_{in}$ and monotonously decreasing with $Q$, as needed.

Practically, if the elements are represented by a lookup function $Q(P_{in}, P_{out})$, their parallel connection becomes especially simple, one just needs to sum the corresponding lookup tables. Sequential connection requires the inversion of the lookup functions, which can be performed on the fly by solving the equation

$$Q_1(P_{in}, P^*) = Q_2(P^*, P_{out}) \quad (14)$$

for the intermediate pressure $P^*$. Here the first function monotonously decreases with $P^*$, while the second function monotonously increases with $P^*$. Also, the continuation of the functions outside working region ensures the following signs at infinities

$$Q_1(P_{in}, \pm\infty) = \mp\infty, \; Q_2(\pm\infty, P_{out}) = \pm\infty. \quad (15)$$

As a result, the graphs of these functions always have a single intersection point, as shown in Figure 7. Thus, equation (14) has a unique solution. It can be found, e.g., by Newton's method with Armijo line search stabilizer. Since lookup functions are piecewise linear with respect to $P^*$, this method converges to the solution in a finite number of steps. Then, the resulting $Q_1(P_{in}, P^*)$ gives a combined diagram $Q(P_{in}, P_{out})$ for the sequential station.

Being equipped with the elementary algorithms for parallel and sequential connections, one can apply them recursively to reduce the compressor station to a single element, also for mixed configurations.

## VI. Generic topological reduction

In exactly the same way, the rules for combining parallel and sequential connections can be applied to the edge elements of an arbitrary type. Suppose that all elements in the network are represented by tabulated lookup functions. Applying the above described parallel and sequential connection rules, one can combine the elements and reduce the network graph significantly. In the given section, we will investigate this possibility. Here, we do not actually implement the tabulation for all elements, instead, we estimate the efficiency of the reduction to forecast a benefit of such implementation.

Parallel and sequential connection rules are based on Kirchhoff's law, which must be modified in supply/exit nodes. The simple summing rule for parallel configuration remains valid also in the presence of such nodes. For sequential configuration modifications of the algorithm are needed.

There are $Q_{set}$ nodes, where source/sink contributions for the flow are given. If an intermediate node in sequential configuration has $Q_{set}$, it should be used to shift one of the flow arguments in $P_{out,2}(P_{out,1}(P_{in}, Q), Q - Q_{set})$, or, equivalently, in the equation $Q_1(P_{in}, P^*) - Q_{set} = Q_2(P^*, P_{out})$. The shifts $Q - Q_{set}$ obviously do not change the signature of the derivatives in the element equation and do not influence the stability.

To keep a standard form of the element with a unique flow assigned to it one can formally define $Q = Q_1$ and move $Q_{set}$ to the output node. Such shifts should be stored so that the inverse reconstruction can return all $Q_{set}$ entries to their places. The algorithm will shift $Q_{set}$ entries until they stop in a node of irreducible skeleton. If two $Q_{set}$ entries collide, their values can be summed. If $Q_{set}$ stops in $P_{set}$ node, it means an addition to the unknown $Q$ source/sink contribution, which is already present there.

In $P_{set}$ nodes Kirchhoff's law is replaced by $P = P_{set}$ condition. If this node appears as the intermediate node in sequential configuration, the element functions $Q_1(P_{in}, P_{set})$ and $Q_2(P_{set}, P_{out})$ can be used to find (generally non-equal) flows. The difference of these flows is sourced/sinked in this $P_{set}$ node.

However, to keep the element standard, one needs to shift the unknown flow contribution to the output node. It cannot be implemented as a standard $Q_{set}$ since this contribution is not a constant but depends on $P_{in}$, $P_{out}$. Therefore, the topological reduction should be stopped in $P_{set}$ nodes.

Practically, the algorithm can be also stopped in the other user-defined nodes. One can agglomerate passive subgraphs, e.g., consisting of pipes and resistors, and keep $P_{set}$, $Q_{set}$, compressors, regulators and other active elements noncontracted. In this way, a significant reduction can be achieved while the state of active elements and all values defining scenario settings remain under user control.

In particular cases, further simplifications are possible. Electric elements depend on voltage difference and require not

2D but 1D profiles. This significantly reduces the computational effort. Linear electric resistors and quadratic hydraulic resistors are described by numerical constants instead of profiles, bringing an additional speedup.

Our non-linear element equations are similar to Green's functions [20] in linear systems measuring a response of the system on an external perturbation. The elements with two ends (edges) are described by two-point Green's functions, which can be properly combined into the other two-point Green's function by parallel and sequential connections. For more complex topologies, higher order response functions can be introduced (three-point, etc.). Technically it is possible to precompute also higher order functions. However, their storage and processing will require introduction of multidimensional tables with enormous consumption of resources and computational expenses. We prefer to stay on two-point level and apply the reduction algorithms there.

It is clear that not all networks can be reduced to a single element by a combination of parallel and sequential (parseq) reduction algorithms. Figure 8 shows some examples of irreducible network topologies. Circular symbols on this figure denote arbitrary, not necessarily identical elements. In the examples shown in Figure 8a-d,g neither parallel nor sequential connections can be found and the networks cannot be further reduced by these algorithms. An exception is the case when the vertical elements in the configurations Figure 8a,b are closed or open valves, or shortcuts. Then these configurations become further reducible.

An additional resource for the reduction is available for tree-like subgraphs, as shown in Figure 8c,d. Suppose that the leaves of the tree (nodes of valency 1) are all $Q_{set}$ nodes, including the regular $Q_{set} = 0$ ones. An exception is one node (the root), which is either $P_{set}$ node or it is connected to a larger parent graph. For definiteness, on Figure 8c,d, the leftmost node can be considered as the root.

Using Kirchhoff's law, one can sum the flows starting from leaves towards the root and completely determine the flow distribution in this subgraph. Then, starting from the root and using element functions in the form $P_{out}(P_{in}, Q)$, one can transfer $P$-values upto the leaves. In this way, the problem can be solved in the subgraph by a simple algorithm without actually passing it to the generic solver. On the topological level, the whole tree-like subgraph can be collapsed to the root node, representing a cumulative $Q_{set}$ for this subgraph, in frames of the parent graph.

The tree reduction algorithm is essentially based on the presence of a single $P_{set}$ node in the subgraph. If the tree contains two or more $P_{set}$ nodes, Kirchhoff's law cannot be applied and the reduction algorithm stops there. The reduction can also require the combination of all algorithms. On Figure 8e one needs to apply parallel reduction to proceed with the tree. On Figure 8f the graph can be reduced by application of sequential, parallel and tree algorithm. On Figure 8g one needs to apply tree algorithm first, then parseq.

It is remarkable that namely the operations of parallel/sequential elimination and tree reduction, which in our application simplify the numerical solution of network problems, are used in graph theory to accelerate the solution of combinatorial problems, upto linear time performance. In our case, the elimination of subgraphs of SPG/GSPG type [15], [16] allows to reduce the network to a skeleton, on which the actual numerical solution should be performed. Then the solution in the reduced parts can be reconstructed back by simple algorithms.

In our implementation, the topological reduction procedure starts from a common algorithm (clean), performing the following steps. All closed elements (closed valves, compressors, regulators) are removed from the network together with disconnected subgraphs where no $P_{set}$ is reachable. This step ensures that $P$-values are everywhere defined. All open elements (open valves, shortcuts, short segments of pipes, compressors and regulators in bypass mode, etc.) that transfer $P$-values from one node to the other without a change are collapsed. This step ensures that no superconductive loops appear leading to cycles of undefined flow. The both steps are necessary to provide global non-degeneracy of the system.

Then parallel, sequential and tree algorithms are applied one after the other, repeatedly, till the reduction is complete. The reduced graph is passed to the solver. After the solution is found, the reduction history can be used to recover the complete answer.

We remind that the last step in the reduction procedure was either a join of two elements, parallel or sequential, or elimination of the leaf. If it was parallel join, $P_{in}, P_{out}$ are common, $Q$ is known, while $Q_1/Q_2$ balance can be found using stored $Q_1(P_{in}, P_{out}), Q_2(P_{in}, P_{out})$ characteristics. If it was sequential join, $Q$ is common, $P_{in}, P_{out}$ are known, the intermediate value $P^*$ can be reconstructed using stored $P_{out,2}(Q, P_{in})$. If it was elimination of the leaf, $Q$ and $P_{in}$ are known, $P_{out}$ can be found from the stored $P_{out}(Q, P_{in})$. Thus, we have recovered the missed properties in one step and can repeat this process recursively until all these data are reconstructed.

## VII. Results

For benchmarking the algorithms, we have received a number of realistic test scenarios from our industrial partners. The simplest gas transport network N1 from our test set is shown in Figure 1. It contains two compressor stations, each equipped with two machine units, cf. Figure 2 (bottom), working in parallel mode. It has two $P_{set}$ supplies and three $Q_{set}$ consumers. The color shows the pressure distribution over the network, arrows – the direction of gas flow, thickness of lines – the diameter of the pipes. Supplies are shown by rhombi, consumers (n76, n80, n91) are shown by triangles. The main elements are shown in the legend.

A closeup to one of the compressors is shown in Figure 2 (bottom), and its characteristics are displayed in Figure 4 (top). Parameters of more complex networks are presented in Table I. In particular, medium-sized network N2 contains about a thousand nodes and edges and is equipped with 7 compressors. The largest considered network N3 has about five thousand nodes and edges and is driven by 25 compressors. Topological connection of elements in the network together with geographic coordinates, the lengths and diameters of pipes form so called *geometry* of the network. Physical setting, such as supply pressures and consumer flows, control settings of compressors and regulators, define *scenario* for the particular simulation case. All networks in our test set were simulated with the same gas composition at 20°C environmental temperature.

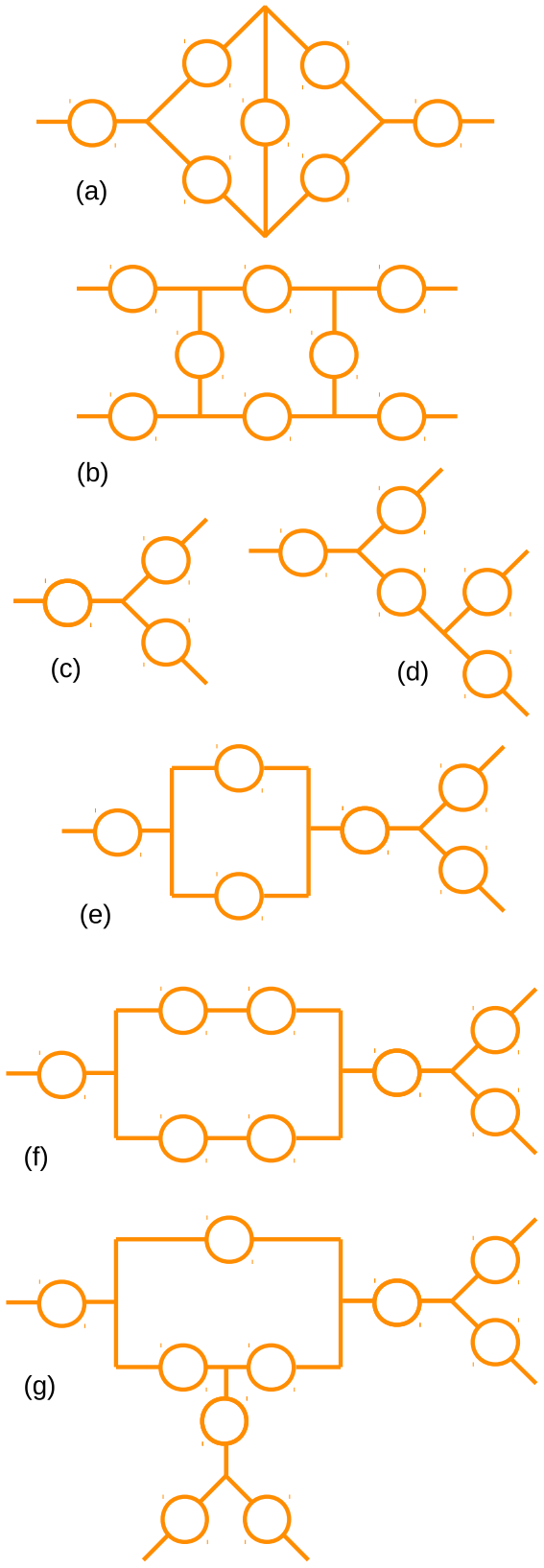


Figure 8. Examples of network topologies: (a-d) are irreducible for parseq algorithm, (c,d) are reducible for tree algorithm, (e-g) require combination of algorithms parseq+tree.

TABLE I. PARAMETERS OF TEST NETWORKS

| network | nodes | edges | compressors | psets |
|---|---|---|---|---|
| N1 | 100 | 111 | 4 | 2 |
| N2 | 931 | 1047 | 7 | 4 |
| N3 | 4466 | 5362 | 25 | 6 |

In Table II, we compare the performance of the implemented algorithms (strategy “stable”) with the performance of the solver with standard settings. For each network in the test set two scenarios are considered, with different numerical values of set points for input pressures and output flows and compressor/regulator $SM$, $SPO$ settings. Divergent cases are marked as ’div’. The number of iterations (iter.) and timing (t) are given. The simulation is performed on a 3 GHz Intel i7 CPU 8 GB RAM workstation.

All scenarios are tested both with free and advanced compressor models. We see that the standard solver provides worse convergence and even diverges in certain scenarios. Some scenarios show divergence already for free compressors, some diverge on advanced ones only. The new algorithm converges in all cases, in agreement with its theoretical properties. We also see that the table lookup implemented for advanced modeling has a negligible computational overhead in strategy “stable”.

TABLE II. COMPARISON OF THE ALGORITHMS

| scenario | solver_strategy | | | | | | | |
|---|---|---|---|---|---|---|---|---|
| | standard | | | | stable | | | |
| | free | | advanced | | free | | advanced | |
| | iter. | t, sec | iter. | t, sec | iter. | t, sec | iter. | t, sec |
| N1S1 | 3 | 0.01 | 32 | 0.12 | 2 | 0.01 | 2 | 0.01 |
| N1S2 | 57 | 0.17 | 70 | 0.21 | 11 | 0.03 | 4 | 0.02 |
| N2S1 | 11 | 0.27 | 19 | 0.64 | 12 | 0.31 | 12 | 0.37 |
| N2S2 | div | – | div | – | 13 | 0.36 | 15 | 0.48 |
| N3S1 | div | – | div | – | 26 | 3.3 | 23 | 3.5 |
| N3S2 | 47 | 6.5 | div | – | 26 | 3.3 | 24 | 3.6 |

TABLE III. NODES / EDGES COUNT FOR REDUCTION ALGORITHMS

| network | orig | clean | clean+ parseq | clean+ parseq+tree |
|---|---|---|---|---|
| N1 | 100 / 111 | 37 / 38 | 10 / 9 | 2 / 1 |
| N2 | 931 / 1047 | 504 / 514 | 289 / 295 | 15 / 17 |
| N3 | 4466 / 5362 | 1755 / 1843 | 1012 / 1056 | 46 / 62 |

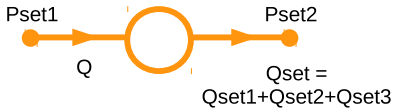


Figure 9. Network N1 after topological reduction.

The network N1, whose original structure is displayed on Figure 1, is ultimately reduced to a single element directly connecting two $P_{set}$ nodes, see Figure 9. The element equation immediately allows to find the flow through the element: $Q(P_{set1}, P_{set2})$. All $Q_{set}$ nodes are moved by the algorithm to the output node, into $P_{set2}$. The value $Q(P_{set1}, P_{set2}) - Q_{set}$ defines the flow sourced / sinked in this node. The inverse reconstruction procedure will redistribute the cumulative $Q_{set}$ to the actual positions.

In Table III, the efficiency of the topological reduction algorithms applied to the test networks is presented. Already the first step (clean) brings significant reduction, due to the abundance of valves and shortcuts in the network. Further steps bring a significant reduction factor ∼70. Therefore, the reduced networks will be solved very fast or will have an explicit solution, like N1 example above. However, one should not forget that the reduction procedure includes operations on the data fields, large tables and is computationally intensive.

Estimation shows that topological reduction requires $O(N_{it1}N_{px}^2N_{elem})$ operations and $O(N_{px}^2N_{elem})$ memory, where $N_{it1}$ is an average number of iterations per pixel necessary to to combine two neighbor elements, $N_{px}$ is the resolution of element diagrams, $N_{elem} = N + E$ is the total number of elements. The practical values are $N_{it1}$ ∼1-10, $N_{px}$ ∼10-100. The direct solution also has an empirical estimation of $O(N_{it2}b^2N_{elem})$ operations, with $N_{it2}$ ∼10-100, $b$ ∼10-100. Here $N_{it2}$ is the number of iterations of the non-linear solver, bandwidth parameter $b$ is related with the sparsity of the system. The inverse reconstruction requires only lookup operations on stored reduction history and is performed much faster than the forward reduction algorithm.

According to this estimation, the topological reduction is a bit faster than the direct solution, but of the same order of magnitude. Both procedures are linearly scaled with $N_{elem}$. It is important that the topological reduction of certain subsystems can be performed once if their parameterization will not be further changed. Also, the reduction of the system leads to elimination of degenerate degrees of freedom and increases the stability of solution procedure as a whole.

## VIII. Conclusion and Further Plans

A mathematical modeling of gas compressors with their individually calibrated physical profiles has been presented. The measured profiles are converted to an explicitly resolved form using the algorithms inspired by computer graphics. The control element equation for a free compressor has been extended by a lookup function representing the working region of the advanced compressor.

The resulting equation possesses the desired signature of derivatives necessary for global non-degeneracy of the Jacobi matrix. Therefore, the globally convergent algorithm earlier developed for the solution of network problems is also applicable for advanced modeling, with a negligible computational overhead. The efficiency of the approach has been demonstrated for a number of real-life network scenarios. The algorithm significantly overperforms a standard Newtonian solver in terms of stability, number of iterations and computational time.

The algorithms for topological reduction of compressor stations with parallel and sequential connections have been developed. The algorithms combine the lookup tables for individual compressors into a cumulative working diagram, representing the behavior of compressor station as a whole. This allows to eliminate the internal degrees of freedom, further improving numerical stability of the solver.

The topological reduction has been extended by a tree reduction algorithm and its applicability to generic networks of arbitrary elements has been investigated. Estimations of the efficiency of the reduction procedure on realistic network problems shows a potential of significant simplification, with a reduction factor about 70. In certain cases the network appears to be reducible to a single element, thus the solution by the non-linear solver in these cases is actually not needed and the result can be completely reconstructed by simple algorithms from the reduction history.

Our further plans include the implementation of the algorithms with GPU parallelization, extension of compressor profiles with dependencies on temperature and gas composition and a special consideration for nearly singular element equations.

## Acknowledgment

We are grateful to the organizers and participants of INFOCOMP 2017 conference for fruitful discussions. This work is supported by German Federal Ministry for Economic Affairs and Energy, project BMWI-0324019A, MathEnergy: Mathematical Key Technologies for Evolving Energy Grids. This material is also based upon work supported by the German Bundesland North Rhine-Westphalia using fundings from the European Regional Development Fund, grant Nr. EFRE-0800063, project ES-FLEX-INFRA.

## References

[1] T. Clees, I. Nikitin, and L. Nikitina, “Advanced Modeling of Gas Compressors for Globally Convergent Stationary Network Solvers”, in Proc. INFOCOMP 2017, The Seventh International Conference on Advanced Communications and Computation, June 25-29, 2017, Venice, Italy, IARIA, 2017, pp. 52-57.

[2] T. Clees, I. Nikitin, and L. Nikitina, “Making Network Solvers Globally Convergent”, Advances in Intelligent Systems and Computing, vol. 676, 2017, pp. 140-153.

[3] T. Clees, N. Hornung, I. Nikitin, and L. Nikitina, “A Globally Convergent Method for Generalized Resistive Systems and its Application to Stationary Problems in Gas Transport Networks”, In Proc. SIMULTECH 2016, SCITEPRESS, 2016, pp. 64-70.

[4] T. Clees et al., “MYNTS: Multi-phYsics NeTwork Simulator”, In Proc. SIMULTECH 2016, SCITEPRESS, 2016, pp. 179-186.

[5] M. Schmidt, M. C. Steinbach, and B. M. Willert, “High detail stationary optimization models for gas networks”, Optimization and Engineering, vol. 16, num.1, 2015, pp. 131-164.

[6] J. Mischner, H.G. Fasold, and K. Kadner, System-planning basics of gas supply, Oldenbourg Industrieverlag GmbH, 2011 (in German).

[7] J. Nikuradse, “Laws of flow in rough pipes”, NACA Technical Memorandum 1292, Washington, 1950.

[8] C. F. Colebrook and C. M. White, “Experiments with Fluid Friction in Roughened Pipes”, in Proc. of the Royal Society of London, Series A, Mathematical and Physical Sciences, vol. 161, num. 906, 1937, pp. 367-381.

[9] J. Saleh, ed., Fluid Flow Handbook, McGraw-Hill Handbooks, McGraw-Hill, 2002.

[10] DIN EN ISO 12213-2: Natural Gas – Calculation of compression factor, European Committee for Standartization, 2010.

[11] A. Wächter and L. T. Biegler, “On the implementation of an interior-point filter line-search algorithm for large-scale nonlinear programming”, Mathematical Programming, vol. 106, num. 1, 2006, pp. 25-57.

[12] R. Fletcher, Practical Methods of Optimization, Wiley, 2013.

[13] M. Schmidt, M. C. Steinbach, and B. M. Willert, “High detail stationary optimization models for gas networks: validation and results”, Optimization and Engineering online, 2015, DOI: 10.1007/s11081-015-9300-3

[14] A. Griewank, J.-U. Bernt, M. Radons, and T. Streubel, ‘Solving piecewise linear systems in abs-normal form”, Linear Algebra and its Applications, vol. 471, 2015, pp. 500-530.

[15] D. Eppstein, “Parallel recognition of series-parallel graphs”, Information and Computation, vol. 98, 1992, pp. 41-55.

[16] N. M. Korneyenko, “Combinatorial algorithms on a class of graphs”, Discrete Applied Mathematics, vol. 54, 1994, pp. 215-217.

[17] K. Takamizawa, T. Nishizeki, and N. Saito, “Linear-time computability of combinatorial problems on series-parallel graphs”, JACM, vol. 29, 1982, pp. 623-641.

[18] M. W. Bern, E. L. Lawler, and A. L. Wong, “Linear-time Computation of Optimal Subgraphs of Decomposable Graphs”, J. Algorithms, vol. 8, 1987, pp. 216-235.

[19] T. Kikuno, N. Yoshida, and Y. Kakuda, “A Linear Algorithm for the Domination Number of a Series Parallel Graph”, Disc. Appl. Math., vol. 5, 1983, pp. 299-311.

[20] M. Hazewinkel, ed., “Green function”, Encyclopedia of Mathematics, Springer 2001.